Quenching of the Magnetic Moment of a Transition Metal Dopant in Silver Clusters

E. Janssens,[1] S. Neukermans,[1] H. M. T. Nguyen,[2] M. T. Nguyen,[2] and P. Lievens[1,*]

[1]*Laboratorium voor Vaste-Stoffysica en Magnetisme, Katholieke Universiteit Leuven, Celestijnenlaan 200D, B-3001 Leuven, Belgium*
[2]*Afdeling Kwantumchemie, Katholieke Universiteit Leuven, Celestijnenlaan 200F, B-3001 Leuven, Belgium*

(Received 6 December 2004; published 21 March 2005)

Single magnetic atoms embedded in a nonmagnetic host exhibit the Kondo effect in the bulk limit, while in very small molecules the magnetic atom is hardly affected by the matrix. In a combined theoretical (density functional theory) and experimental (photofragmentation and mass spectrometry) study we consider the intermediate case of nanometer sized transition-metal–doped silver clusters. In particular, we provide experimental evidence for enhanced stability of the cobalt-doped silver cluster $Ag_{10}Co^+$ and show theoretically that it has a symmetric endohedral geometry with a closed 18-electron singlet electronic shell structure. This implies that the magnetic moment on the cobalt atom is quenched.

DOI: 10.1103/PhysRevLett.94.113401 PACS numbers: 36.40.Cg, 36.40.Qv, 72.15.Qm, 73.22.–f

One of the long standing problems in condensed matter physics is the behavior of nonmagnetic metals incorporating a low concentration of magnetic atoms. In bulk metals, spin exchange scattering of conduction electrons at the magnetic impurities leads to the formation of a nonmagnetic state at low temperatures, the so-called Kondo effect [1]. While in macroscopic systems the screening cloud extends quite far, this is altered in physically confined systems such as elliptical quantum corrals [2], quantum dots [3,4], and carbon nanotube systems [5]. In these atomic scale systems both the impurity spin and the number of electrons are well controlled.

In this paper we present a system with an ultimately confined and well controlled electron cloud: a single magnetic atom embedded in subnanometer sized silver clusters. The number of silver atoms in the cluster determines the number of itinerant electrons that are interacting with the impurity. For specific cluster sizes the spin of the magnetic atom is completely quenched. The mechanism responsible for this quenching is the formation of closed electron shells, analogous to organometallic compounds complying with the 18-electron rule [6].

As has been demonstrated abundantly for a number of simple metal clusters, specific features, such as intensity maxima and steps in the observed size dependent intensities in mass spectrometric investigations, provide evidence for stabilities enhanced with respect to neighboring sizes [7]. As described by cluster shell models, itinerant electrons are confined in a potential well stemming from the cluster core ions, and occupy a progression of single particle levels, which resemble the spherical harmonics: $1s^2/1p^6/1d^{10}/2s^2/1f^{14}/2p^6/1g^{18}\ldots$ An enhanced stability occurs for sizes corresponding to a number of delocalized (itinerant) electrons that completely fill electron shells: 2, 8, 18, 20, 34, 40, 58, …, the so-called magic numbers. The determining influence of shells of electrons on the properties of metal clusters is well established for alkali, coinage, and trivalent metals [7] and has been corroborated by a number of models with different degrees of sophistication [8]. The situation becomes more complex in the case of alloy clusters consisting of magnetic and nonmagnetic elements, for which theoretical studies have shown that the structure of the cluster influences the electronic and magnetic properties [9–12].

Here, we consider the size and composition dependent stability of bimetallic clusters composed of silver (Ag) and the $3d$ transition metals (X = Sc, Ti, V, Fe, Co, and Ni),

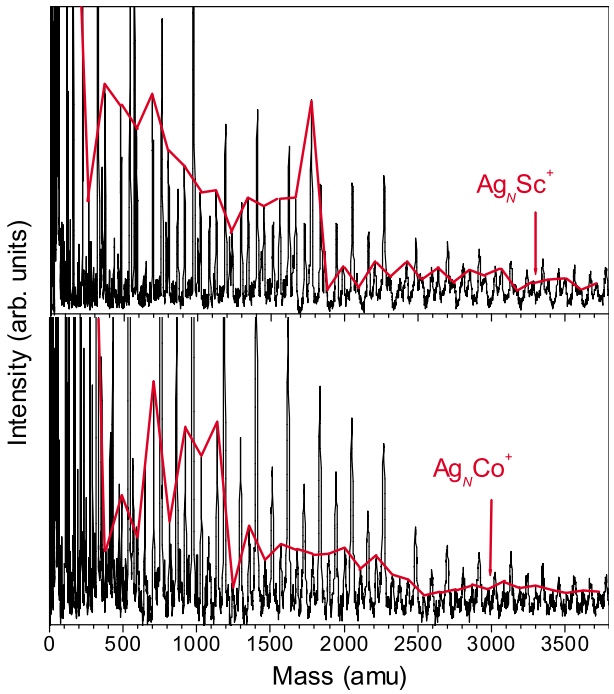

FIG. 1 (color online). Mass spectra showing cluster intensities for $Ag_NSc_M^+$ and $Ag_NCo_M^+$ after photofragmentation with high fluence ArF excimer laser light (>2 MW/cm^2, λ = 193 nm). The clusters containing one dopant atom (M = 1) are connected by a gray line (red online). Intensity maxima and steps in the observed pattern correspond to clusters having enhanced stabilities with respect to neighboring sizes.

which are produced using a dual-target dual-laser vaporization source [13]. The relative stability of singly doped $Ag_N X^+$ clusters follows from photofragmentation mass spectrometry [14]. Intense laser light is used to irradiate and highly excite the produced clusters, and mass spectrometry allows identification of the resulting photoionized fragments. Mass spectra of $Ag_N Sc^+$ and $Ag_N Co^+$ ($N < 30$) clusters are given in Fig. 1, while Fig. 2 shows the size dependence of the measured abundance of photofragmented singly doped species (derived from the mass spectra).

A detailed analysis of the stability patterns of the doped silver clusters allows the identification of a one-to-one correspondence between observed stability features and closed shells. Most of the observed peaks and steps relate to clusters having closed shells of electrons, i.e., a magic number of itinerant electrons. For instance, apparent steps in the mass abundance patterns after Ag_6Sc^+, $Ag_{16}Sc^+$, $Ag_{15}Ti^+$, and $Ag_{14}V^+$ correspond to the magic numbers 8 and 18, provided that Sc, Ti, and V delocalize their valence $4s$ and $3d$ electrons, and each silver atom contributes its one valence $5s$ electron (minus one because cationic clusters are considered). Several other steps or peaks in the mass abundance patterns can be linked with known spherical magic numbers if only the valence s electrons of both dopant and silver atoms are considered to be itinerant. For example, steps after Ag_7Ti^+, Ag_7V^+, and Ag_7Fe^+ correlate with the magic number eight (the amount of dopant s electrons is one or two, depending on the kind of host and on the cluster size) and those after $Ag_{20}Fe^+$, $Ag_{20}Co^+$, and $Ag_{21}Ni^+$ link with the magic number 20. Summarizing, a large number of the apparent stability features in the mass spectra can be interpreted as corresponding to closed shells of electrons if the valence s electrons are considered itinerant. Only for the lightest dopant atoms (Sc, Ti, and V) the valence d electrons might also have to be taken into account.

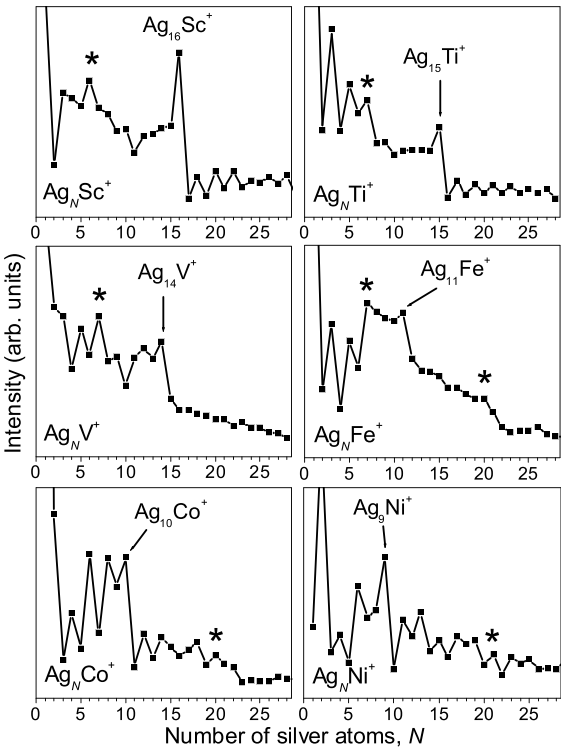

FIG. 2. Measured cluster intensities after photofragmentation as a function of size for $Ag_N X^+$ (X = Sc, Ti, V, Fe, Co, and Ni; $N < 30$). The most pronounced features in these graphs are steps in intensity after the clusters $Ag_{16}Sc^+$, $Ag_{15}Ti^+$, $Ag_{14}V^+$, $Ag_{11}Fe^+$, $Ag_{10}Co^+$, and Ag_9Ni^+, and correlate with a magic number of 18 delocalized electrons. Other smaller intensity drops can be identified as corresponding to the magic numbers eight and 20, and are marked with an asterisk.

So far, these features and interpretations are very analogous to what was observed in a similar investigation of transition-metal–doped gold clusters [14–17]. However, there are a few very pronounced exceptions. The most pronounced steps for $Ag_N Fe^+$ and $Ag_N Co^+$ occur for $N = 11$ and $N = 10$ respectively (see Fig. 2), and there is no relation with known magic numbers of electrons in shell models. Intriguingly, these apparently very stable sizes follow a dopant dependent size pattern, along with the most pronounced feature for $Ag_N Sc^+$ ($N = 16$), $Ag_N Ti^+$ ($N = 15$), and $Ag_N V^+$ ($N = 14$), where the phenomenological explanation was based on an itinerant behavior of both the $4s$ and $3d$ dopant atom electrons. Pursuing this argumentation, the Fe and Co atom in $Ag_{11}Fe^+$ and $Ag_{10}Co^+$ would delocalize 8 and 9 electrons, respectively. In all these cationic transition-metal–doped clusters, this yields a total of 18 electrons, which is a magic number for delocalized electrons filling the $1s$, $1p$, and $1d$ spherical levels in the shell model [7,8].

While at first glance itinerant behavior for all the d electrons seems unrealistic, it does point to a conceptually very similar, and in organometallic chemistry widely applied, interpretation of the electronic structure. The 18-electron rule predicts organometallic compounds of transition metals to be stable and diamagnetic when the valence shell of the metal atom contains 18 electrons [6]. A transition metal atom has nine valence atomic orbitals (five nd, one $(n+1)s$, and three $(n+1)p$), which can be filled by 18 electrons. Also, the manifestation of a similar behavior in highly symmetric transition-metal–doped endohedral clusters has been theoretically predicted: the icosahedral clusters $Cu_{12}Cr$ [18], $Ag_{12}Cr$ [19], $Au_{12}Cr$ [20], $Au_{12}W$ [21], and the D_{6h} cluster $Si_{12}Cr$ [22], all comply with the 18-electron rule. In all these cases, the 18 valence electrons form a closed electronic structure.

Detailed quantum chemical calculations were performed to identify both geometry and electronic structure of $Ag_{10}Co^+$, and furthermore to gain insight in the interplay between the electron cloud of valence electrons and the magnetic impurity. Geometry optimizations and electronic structure calculations were carried out with density functional theory at the generalized gradient approach level using the Becke exchange [23] and the Perdew cor-

relation [24] functional (BP86). The Slater-type orbital basis sets including triple-zeta plus polarization functions (TZVPP) [25] were used for the valence orbitals of Co and Ag. The 28 core electrons of Ag were replaced by a scalar relativistic effective core potential [26], 19 valence electrons are treated explicitly. To optimize the geometry of $Ag_{10}Co^+$ we started from the isomers found for pure silver Ag_{11}^+ taken from Ref. [27] in which nonsymmetry equivalent silver atoms were replaced by a cobalt atom. Both singlet and triplet states were considered, and for singlet states we looked at both closed-shell and open-shell configurations. The nature of the lower-lying minima was verified by a calculation of vibrational frequencies at the BP86-TZ2P level. All geometry optimizations were accomplished with the TURBOMOLE program [28]. While for clusters of this size it is nearly impossible to investigate all possible structures, the detailed search we performed gives us confidence that the global energy minimum has been localized.

Figure 3 shows the identified structures and symmetries, their energy relative to the ground state, and the energy difference between triplet and singlet spin states optimized for each isomer. The lowest energy isomers, including the ground state with a C_s geometry only slightly distorted from D_{4d}, correspond to clusters in which the cobalt is situated at the center of a symmetric Ag_{10} cage, yielding relatively short distances to all surrounding Ag atoms (the Ag-Co bond lengths range between 2.56 and 2.63 Å). Less symmetric isomers in which cobalt locates at a more exterior position are energetically not favorable. It is important to note that the triplet-singlet energy gap, $\Delta E(T-S)$, was always found to be positive for the preferred endohedral isomers (see Fig. 3), identifying the electronic state of these clusters as a singlet. In addition, the large highest-occupied-molecular-orbital–lowest-unoccupied-molecular-orbital gap of 1.43 eV for the obtained ground state constitutes theoretical evidence for the high stability of this cluster, in correspondence with the experimental findings.

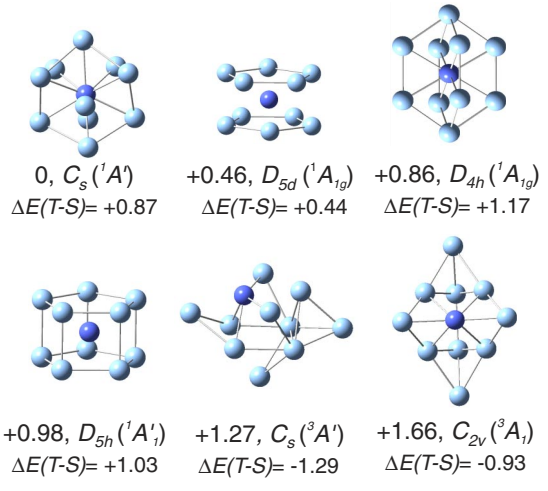

FIG. 3 (color online). Optimized isomers for $Ag_{10}Co^+$ calculated with density functional theory at the BP86-TZVPP level of theory. Relative energies (in eV), symmetries, and singlet-triplet energy gaps ($\Delta E(T-S)$, in eV) are given. The lowest energy isomer (C_s) is only slightly distorted from D_{4d}. The low lying isomers are endohedral (cobalt in the center of a symmetric Ag_{10} cage) and prefer singlet spin states.

An enhanced stability related to the 18-electron rule also can explain the high abundances observed for $Ag_{16}Sc^+$, $Ag_{15}Ti^+$, $Ag_{14}V^+$, and $Ag_{11}Fe^+$ (see Fig. 2). This behavior is not observed for $Ag_{13}Cr^+$ and $Ag_{12}Mn^+$, which might be related to the small *s*-*d* hybridization in these systems because of the enhanced stability of the half filled 3*d* shell in chromium and manganese [29].

In Kondo systems a spin-polarized cloud is built around the magnetic impurity resulting in a singlet state at temperatures below T_K with $k_B T_K$ of the order of $\Delta E(T-S)$. For finite-size systems, like small clusters, hybridization and singlet formation strongly depend on the cluster size or on the number of valence electrons [30]. With the delicate energy balance between Hund's rule and electronic shell closings, it is likely that the quenching of the magnetic

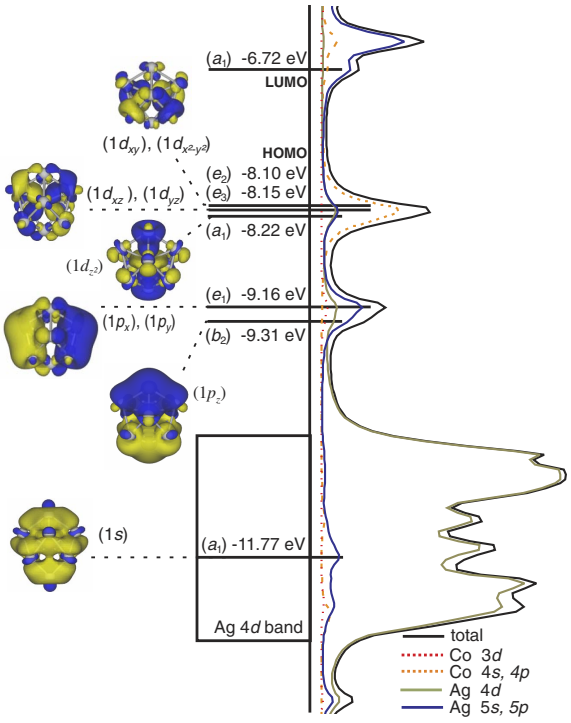

FIG. 4 (color online). Energy levels, density of states, and shapes of the delocalized molecular orbitals of $Ag_{10}Co^+$ (for the isomer with D_{4d} symmetry). The orbitals with e_1, e_2, and e_3 symmetry are twofold degenerate; for these levels only one molecular orbital is presented. The density of states [31,32] shows a large silver *d* band and two bunches of levels near the Fermi level. The five highest occupied levels (the delocalized 1*d* level) are highly hybridized between Ag 5*s*, 5*p*, 4*d* and Co 3*d* electrons. The three lower-lying occupied levels (the delocalized 1*p* level) result from hybridization between Ag 4*d* and Ag 5*s*, 5*p* electrons.

moment at the impurity is induced by the gain in energy related with the 18-electron shell closing. Indeed, the delocalized molecular orbitals of the $Ag_{10}Co^{+}$ ground state structure, presented in Fig. 4, exhibit a strong interaction between the host 5*s* electrons and the magnetic impurity 3*d* and 4*s* electrons. Hybridization of the atomic Ag 5*s* levels with the Co 3*d* levels leads to the formation of delocalized molecular orbitals. The overall shape of the highest occupied orbitals resembles the spherical harmonic functions: 1*s* (one level), 1*p* (three levels) and 1*d* (five levels). The degeneracy of the 1*p*- and 1*d*-like levels is lifted, because of the deviation of the cluster geometry from a perfect sphere. As such the Ag_{10}-cage valence electrons can be considered as forming a spin-compensating electron cloud surrounding the magnetic impurity, somewhat different from, but conceptually very similar to, Kondo physics in larger systems.

In summary we presented the first examples of magnetic-element–doped metal clusters that show a quenching of the impurity magnetic moment for selected sizes. Mass spectrometric investigations showed these clusters to have an enhanced stability. Computations confirmed this high stability and provided evidence for the existence of closed electronic shells in compliance with the 18-electron rule, and a singlet ground state structure with zero magnetic moment. This specific size and composition dependent behavior is analogous to the screening electron cloud formation in magnetic-element–doped bulk metals and therefore can be interpreted as a finite-size precursor of a Kondo system.

This work is supported by the Fund for Scientific Research-Flanders (FWO), the Flemish Concerted Action (GOA/2004/02), and the Belgian Interuniversity Poles of Attraction (IAP/P5/01) programs. E. J. and S. N. thank the FWO for financial support.

*Electronic address: Peter.Lievens@fys.kuleuven.ac.be

[1] J. Kondo, Prog. Theor. Phys. **32**, 37 (1964).
[2] H. C. Manoharan, C. P. Lutz, and D. M. Eigler, Nature (London) **403**, 512 (2000).
[3] S. M. Cronenwett, T. H. Oosterkamp, and L. P. Kouwenhoven, Science **281**, 540 (1998).
[4] S. Sasaki, S. De Franceschi, J. M. Elzerman, W. G. van der Wiel, M. Eto, S. Tarucha, and L. P. Kouwenhoven, Nature (London) **405**, 764 (2000).
[5] J. Nygard, D. H. Cobden, and P. E. Lindelof, Nature (London) **408**, 342 (2000).
[6] R. H. Crabtree, *The Organometallic Chemistry of the Transition Metals* (Wiley, New York, 2001), 3rd ed.
[7] W. A. de Heer, Rev. Mod. Phys. **65**, 611 (1993).
[8] M. Brack, Rev. Mod. Phys. **65**, 677 (1993).
[9] D. Guenzburger and D. E. Ellis, Phys. Rev. Lett. **67**, 3832 (1991).
[10] X. S. Chen, J. J. Zhao, and G. H. Wang, Z. Phys. D **35**, 149 (1995).
[11] D. Bagayoko, P. M. Lam, N. Brener, and J. Callaway, Phys. Rev. B **54**, 12184 (1996).
[12] E. B. Krissinel and J. Jellinek, Int. J. Quantum Chem. **62**, 185 (1997).
[13] W. Bouwen, P. Thoen, F. Vanhoutte, S. Bouckaert, F. Despa, H. Weidele, R. E. Silverans, and P. Lievens, Rev. Sci. Instrum. **71**, 54 (2000).
[14] S. Neukermans, E. Janssens, H. Tanaka, R. E. Silverans, and P. Lievens, Phys. Rev. Lett. **90**, 033401 (2003).
[15] H. Tanaka, E. Janssens, S. Neukermans, R. E. Silverans, and P. Lievens, J. Am. Chem. Soc. **125**, 2862 (2003).
[16] E. Janssens, H. Tanaka, S. Neukermans, R. E. Silverans, and P. Lievens, New J. Phys. **5**, 46 (2003).
[17] E. Janssens, H. Tanaka, S. Neukermans, R. E. Silverans, and P. Lievens, Phys. Rev. B **69**, 085402 (2004).
[18] Q. Sun, X. G. Gong, Q. Q. Zheng, D. Y. Sun, and G. H. Wang, Phys. Rev. B **54**, 10896 (1996).
[19] Q. Sun, Q. Wang, J. Z. Yu, Z. Q. Li, J. T. Wang, and Y. Kawazoe, J. Phys. I **7**, 1233 (1997).
[20] S. Y. Wang, J. Z. Yu, H. Mizuseki, Q. Sun, C. Y. Wang, and Y. Kawazoe, Phys. Rev. B **70**, 165413 (2004).
[21] P. Pyykkö and N. Runeberg, Angew. Chem., Int. Ed. Engl. **41**, 2174 (2002).
[22] S. N. Khanna, B. K. Rao, and P. Jena, Phys. Rev. Lett. **89**, 016803 (2002).
[23] A. D. Becke, Phys. Rev. A **38**, 3098 (1988).
[24] J. P. Perdew, Phys. Rev. B **33**, 8822 (1986).
[25] K. Eichkorn, F. Weigend, O. Treutler, and R. Ahlrichs, Theor. Chem. Acc. **97**, 119 (1997).
[26] D. Andrae, U. Haussermann, M. Dolg, H. Stoll, and H. Preuss, Theor. Chim. Acta **77**, 123 (1990).
[27] P. Weis, T. Bierwieler, S. Gilb, and M. M. Kappes, Chem. Phys. Lett. **355**, 355 (2002).
[28] R. Ahlrichs, M. Bär, H. Horn, and C. Kölmel, Chem. Phys. Lett. **162**, 165 (1989).
[29] E. Janssens, S. Neukermans, X. Wang, N. Veldeman, R. E. Silverans, P. Lievens, Eur. Phys. J. D (to be published).
[30] J. L. Ricardo-Chávez and G. M. Pastor, J. Appl. Phys. **87**, 6800 (2000).
[31] Percentage compositions of molecular orbitals, and density-of-states spectra were calculated using AOMIX: S. I. Gorelsky, computer code AOMIX program, rev. 5.95, http://www.sg-chem.net/.
[32] S. I. Gorelsky and A. B. P. Lever, J. Organomet. Chem. **635**, 187 (2001).